FACULTY OF ELECTRICAL ENGINEERING
KTE
September 10 - 12, 2007
Pilsen, Czech Republic

CONVERGENCE PROBLEMS OF INTEGRAL MODELING OF 3D ELECTROSTATIC FIELDS WITH SINGULARITIES

ING. ROMAN HAMAR, PH.D.
PROF. ING. IVO DOLEŽEL, CSC.

Abstract: *Numerous electrostatic fields are characterized by the presence of singularities (for example, at the corners or along the edges of electrically conductive charged bodies). Solutions to the tasks involving such elements by classic low-order differential methods often lead to inaccurate results. One of the prospective methods seems to be the integral approach starting from finding the distribution of the charge using the system of the first-kind Fredholm equations. The paper shows an application of this approach to two electrically conductive cubes in a general position in space. Discretization of their surfaces is performed in several different ways and the results are compared with respect to their convergence.*

Key words: *Electrostatic field, integral equation, surface charge, numerical analysis*

INTRODUCTION

Even when more than 90 % problems associated with electrostatic fields are nowadays estimated to be solvable by the differential techniques (mostly the finite element method, more rarely by the finite difference technique that is, however, no real competitor), there exist several groups of tasks where the application of these methods may appear problematic. One of them includes finding the distribution of surface electric charge in 3D systems of charged electrically conductive bodies. The main obstacle is here represented by the necessity of discretizing large definition areas including ambient media (air) and possible singularities (the surface charge grows to infinity at every corner or edge of any body in the system).

As far as the number of the bodies under investigation is reasonably small and the system is electrically homogeneous, the integral method may prove to be a powerful and reliable alternative. Its basic ideas are not new, but as not so high attention was paid to this technique in the past, the relevant references are not very numerous [1], [2]. As known, the problem under investigation (finding the distribution of the electric charge on the surfaces of several 3D bodies in an arbitrary position) is described by a set of the first-kind Fredholm integral equations. The numerical solution to this set is, however, relatively complicated and often accompanied by specific difficulties. One of them is manipulation with fully populated matrices and another problem consists in the evaluation of various proper and improper integrals occurring in its coefficients. Local problems with accuracy may also appear, which is associated with a high charge density near various edges, corners etc.

The paper, that represents a natural continuation of previous work [3], deals with the formulation of the basic continuous mathematical model of the problem and possibilities of its numerical solution. The theoretical analysis is illustrated on an example of two electrically conductive cubes in a general position in space. Particular attention is paid to the convergence of results in dependence on the density and arrangement of the discretization mesh.

1 CONTINUOUS MATHEMATICAL MODEL

Consider a system of *n* mutually isolated well conductive metal bodies $\Omega_i, i = 1,\ldots,n$ (see Fig. 1) carrying constant electric potentials $\varphi_i, i = 1,\ldots,n$. The system is placed in a homogeneous medium of permittivity ε_0. Dimensions of the conductors are finite and their surfaces smooth by parts. It is necessary to find the distribution of the charge density over the surfaces of the particular bodies and map the electric field in their vicinity.

Let us choose a reference point $Q_k \in S_k$, where S_k is the surface of body Ω_k. The electric potential φ_k at the point Q_k is given by relation [3]

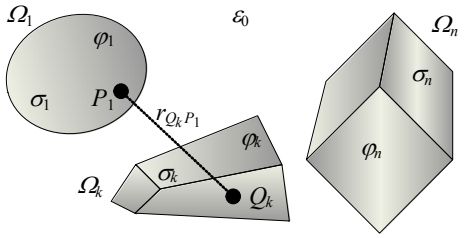

Fig. 1: A general system of n electrically charged bodies

$$\varphi_k\left(Q_k\right)=\frac{1}{4\pi\varepsilon_0}\sum_{i=1}^{n}\int_{S_i}\frac{\sigma_i\left(P_i\right)\mathrm{d}S}{r_{Q_k P_i}}+\varphi_0 \tag{1}$$

where P_i denotes a general integration point $P_i\in\Omega_i$ (the significance of other symbols follows from Fig. 1). The basic advantage of function $1/r_{Q_k P_i}$ is its integrability in 2D. Solvability of the system (1) and unambiguousness of the continuous model was proved in [2].

2 DISCRETIZED MATHEMATICAL MODEL

Let surfaces S_i of the bodies Ω_i, $i=1,\ldots,n$ be approximated by meshes consisting of planar elements. Let N_i denote the number of elements of magnitude T_{ij} covering the surface S_i. No additional assumptions are imposed on the surface meshes as the collocation scheme by which the system (1) is discretised considers only the midpoints and areas of the individual cells. Starting from Fig. 2, where each element is supposed to carry a constant value of the surface charge, the approximate solution to (1) is now given by the equation

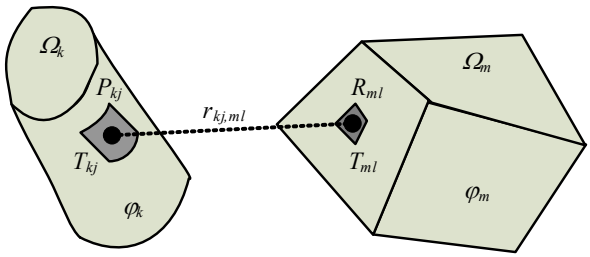

Fig. 2: To the discretized model

$$\varphi_k\left(P_{kj}\right)\approx\frac{1}{4\pi\varepsilon_0}\cdot\sum_{m=1}^{\mathrm{n}}\sum_{l=1}^{\mathrm{N}_m}\sigma_{ml}\int_{T_{ml}}\frac{\mathrm{d}S}{r_{kj,ml}}+\varphi_0 \tag{2}$$
$$k=1,\ldots,n,\ \ j=1,\ldots,N_k$$

where P_{kj} is the midpoint of element $T_{kj}\in S_k$, σ_{ml} is the charge density in element T_{ml} and $r_{kj,ml}$ is the distance between the reference point P_{kj} and a general integration point $R_{ml}\in T_{ml}$.

As the integration constant φ_0 is unknown, the system has to be supplemented by the condition

$$\sum_{m=1}^{\mathrm{n}}\sum_{l=1}^{\mathrm{N}_m}\sigma_{ml}T_{ml}=Q \tag{3}$$

where Q is the total charge of the system.

As far as the elements are of triangular or rectangular types, the integrals

$$\int_{T_{ml}}\frac{\mathrm{d}S}{r_{kj,ml}} \tag{4}$$

can be calculated analytically. Let us illustrate it for a rectangle in Fig. 3 (but this arrangement has to be recalculated for a general position of the rectangle)

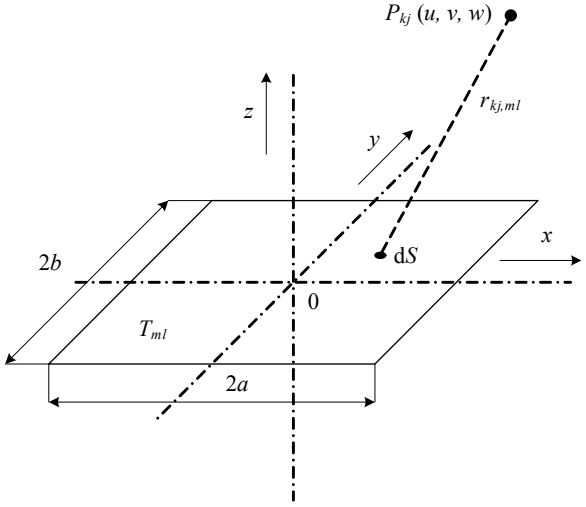

Fig. 3: To the computation of integral $\int_{T_{ml}}\frac{\mathrm{d}S}{r_{kj,ml}}$ over a rectangle

$$\begin{aligned}
&\int_{x=-a}^{a}\int_{y=-b}^{b}\frac{\mathrm{d}y\,\mathrm{d}x}{\sqrt{(x-u)^2+(y-v)^2+w^2}}=\\
&=w\cdot\arctan\frac{(u+a)(v-b)}{w\sqrt{(u+a)^2+(v-b)^2+w^2}}-\\
&-w\cdot\arctan\frac{(u-a)(v-b)}{w\sqrt{(u-a)^2+(v-b)^2+w^2}}-\\
&-w\cdot\arctan\frac{(u+a)(v+b)}{w\sqrt{(u+a)^2+(v+b)^2+w^2}}+\\
&+w\cdot\arctan\frac{(u-a)(v+b)}{w\sqrt{(u-a)^2+(v+b)^2+w^2}}+\\
&+(v-b)\cdot\ln[\sqrt{(u+a)^2+(v-b)^2+w^2}-(u+a)]+\\
&+(u+a)\cdot\ln[\sqrt{(u+a)^2+(v-b)^2+w^2}-(v-b)]-\\
&-(v-b)\cdot\ln[\sqrt{(u-a)^2+(v-b)^2+w^2}-(u-a)]-\\
&-(u-a)\cdot\ln[\sqrt{(u-a)^2+(v-b)^2+w^2}-(v-b)]-\\
&-(v+b)\cdot\ln[\sqrt{(u+a)^2+(v+b)^2+w^2}-(u+a)]-\\
&-(u+a)\cdot\ln[\sqrt{(u+a)^2+(v+b)^2+w^2}-(v+b)]+\\
&+(v+b)\cdot\ln[\sqrt{(u-a)^2+(v+b)^2+w^2}-(u-a)]+\\
&+(u-a)\cdot\ln[\sqrt{(u-a)^2+(v+b)^2+w^2}-(v+b)].
\end{aligned} \tag{5}$$

while for a triangle in Fig. 4 (that is of a sufficiently general type)

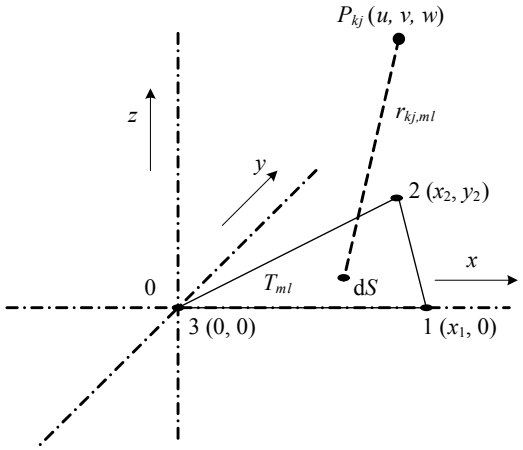

Fig. 4: To the computation of integral $\int_{T_{ml}} \frac{\mathrm{d}S}{r_{kj,ml}}$ *over a general triangle*

Let us introduce first several constants following from the geometry of the arrangement

$$\begin{gathered} A = a,\ B = -b,\ C = A^2 + y_2^2, \\ D = 2AB - 2vy_2,\ G = \frac{vA + y_2 B}{A^2 + y_2^2} + w^2, \\ P = \frac{A}{\sqrt{C}},\ Q = B - \frac{AD}{2C}, \\ s_1 = \frac{D}{2\sqrt{C}},\ s_2 = \frac{2C + D}{2\sqrt{C}}. \end{gathered} \tag{6}$$

Then, after laborious and time consuming computation we get

$$\begin{aligned} \int_{T_{ml}} \frac{\mathrm{d}S}{r_{kj,ml}} &= \frac{y_2}{\sqrt{C}}\left(s_2 + \frac{PQ}{P^2-1}\right)\ln\left(Ps_2 + Q + \sqrt{s_2^2 + G}\right) - \\ &- \frac{s_2 \cdot y_2}{\sqrt{C}} - \frac{Qy_2}{P^2-1}\ln\left(\frac{s_2 + \sqrt{s_2^2 + G}}{\sqrt{G}}\right) + \\ &+ \frac{2y_2\sqrt{G\left(1-P^2\right) - Q^2}}{\left(P^2-1\right)\sqrt{C}} \cdot \\ &\cdot \arctan \frac{\left(Q - \sqrt{G}\right)\dfrac{\sqrt{s_2^2 + G} - \sqrt{G}}{s_2} - \sqrt{G}P}{\sqrt{G\left(1-P^2\right) - Q^2}} - \\ &- \frac{y_2}{\sqrt{C}}\left(s_1 + \frac{PQ}{P^2-1}\right)\ln\left(Ps_1 + Q + \sqrt{s_1^2 + G}\right) + \\ &+ \frac{s_1 \cdot y_2}{\sqrt{C}} + \frac{Qy_2}{P^2-1}\ln\left(\frac{s_1 + \sqrt{s_1^2 + G}}{\sqrt{G}}\right) - \\ &\frac{2y_2\sqrt{G\left(1-P^2\right) - Q^2}}{\left(P^2-1\right)\sqrt{C}} \cdot \end{aligned}$$

$$\cdot \arctan \frac{\left(Q - \sqrt{G}\right)\dfrac{\sqrt{s_1^2 + G} - \sqrt{G}}{s_1} - \sqrt{G}P}{\sqrt{G\left(1-P^2\right) - Q^2}}. \tag{7}$$

Both expressions (5) and (7) have finite limits for $w = 0$ (reference point P_{kj} is placed in the plane of the element). Their values are for the rectangle

$$\begin{aligned} &\int_{x=-a}^{a}\int_{y=-b}^{b} \frac{\mathrm{d}y\,\mathrm{d}x}{\sqrt{(x-u)^2 + (y-v)^2}} = \\ &= (v-b)\cdot\ln\left[\frac{\sqrt{(u+a)^2 + (v-b)^2} - (u+a)}{\sqrt{(u-a)^2 + (v-b)^2} - (u-a)}\right] + \\ &+ (u+a)\cdot\ln\left[\frac{\sqrt{(u+a)^2 + (v-b)^2} - (v-b)}{\sqrt{(u+a)^2 + (v+b)^2} - (v+b)}\right] - \\ &+ (v+b)\cdot\ln\left[\frac{\sqrt{(u-a)^2 + (v+b)^2} - (u-a)}{\sqrt{(u+a)^2 + (v+b)^2} - (u+a)}\right] + \\ &+ (u-a)\cdot\ln\left[\frac{\sqrt{(u-a)^2 + (v+b)^2} - (v+b)}{\sqrt{(u-a)^2 + (v-b)^2} - (v-b)}\right]. \end{aligned} \tag{8}$$

and for $u = v = 0$, which is the most common case

$$\begin{aligned} &\int_{x=-a}^{a}\int_{y=-b}^{b} \frac{\mathrm{d}y\,\mathrm{d}x}{\sqrt{x^2 + y^2}} = \\ &= 2b\cdot\ln\left[\frac{\sqrt{a^2 + b^2} + a}{\sqrt{a^2 + b^2} - a}\right] + 2a\cdot\ln\left[\frac{\sqrt{a^2 + b^2} + b}{\sqrt{a^2 + b^2} - b}\right] \end{aligned} \tag{9}$$

Analogously, for a triangle we have ($w = 0$)

$$\begin{aligned} \int_{T_{ml}} \frac{\mathrm{d}S}{r_{kj,ml}} &= \frac{y_2}{\sqrt{C}}\left(s_2 + \frac{PQ}{P^2-1}\right)\ln\left(Ps_2 + Q + \sqrt{s_2^2 + G}\right) - \\ &- \frac{s_2 \cdot y_2}{\sqrt{C}} - \frac{Qy_2}{P^2-1}\ln\left(\frac{s_2 + \sqrt{s_2^2 + G}}{\sqrt{G}}\right) - \\ &\frac{y_2}{\sqrt{C}}\left(s_1 + \frac{PQ}{P^2-1}\right)\ln\left(Ps_1 + Q + \sqrt{s_1^2 + G}\right) + \\ &+ \frac{s_1 \cdot y_2}{\sqrt{C}} + \frac{Qy_2}{P^2-1}\ln\left(\frac{s_1 + \sqrt{s_1^2 + G}}{\sqrt{G}}\right) \end{aligned} \tag{10}$$

where the constants are given by (6).

3 ILLUSTRATIVE EXAMPLE

The method was tested on two charged cubes in a general position (see Fig. 5) placed in the air. The length of the edge of both cubes is 0.02 m and the distance of

their centers 0.035 m. The electric potential of the left cube is $\varphi_1 = -50$ V, of the right cube $\varphi_2 = 50$ V. Fig. 5 also contains several reference points $(1, 2, \ldots, 6)$ at which we tested some important field quantities.

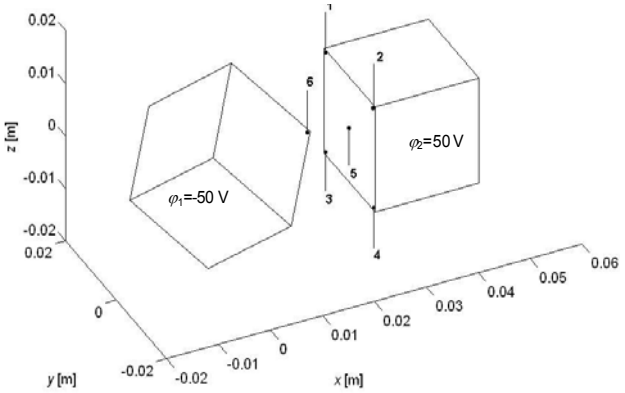

Fig. 5: The investigated arrangement of both cubes

The computations were carried out on nonuniform rectangular grids whose elements decreased towards the edges and corners in order to ensure more realistic distribution of the surface electric charge. The number of rectangular elements covering one face grew from $36\,(6\times6)$ elements to $400(20\times20)$ elements. In the last case the number of the degrees of freedom was $400\times12 = 4800$, which represents the limit of capabilities of the used PC. Moreover, the nonuniform grid was created by several ways.

The computations provided a lot of results. There will be presented several of those obtained on a grid, whose elements (as to their area) decreased parabolically towards the edges of the face.

To illustrate, Fig. 6 shows the distribution of the surface charge in the system for 400 rectangular elements in every face.

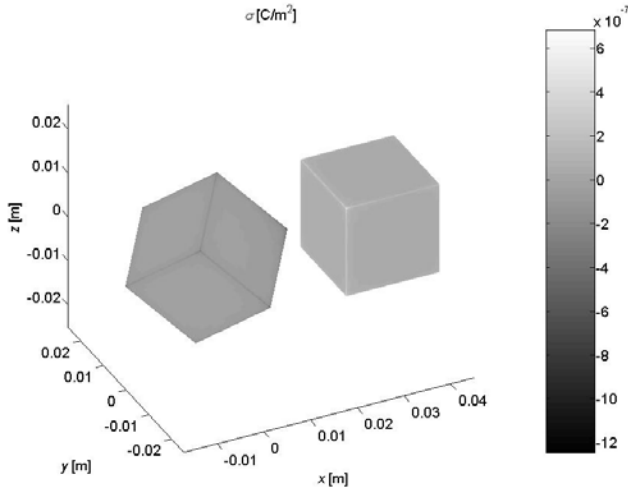

Fig. 6: Distribution of the surface charge in the system (the number of elements in every face being 400)

The highest density may really be observed along the particular edges of both cubes. From the distribution of charge (on the same grid) we calculated the distribution of electric field near both cubes. This distribution is depicted in Fig. 7.

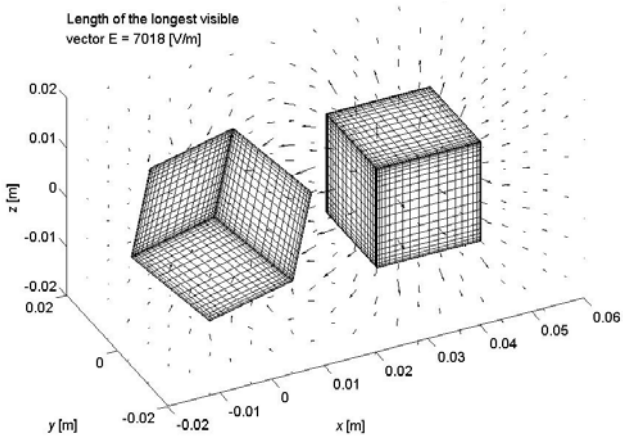

Fig. 7: Distribution of electric field near the cubes

Fig. 8 shows the distribution of potential and module of the electric field strength along the abscissa connecting points 5 and 6 (see Fig. 5).

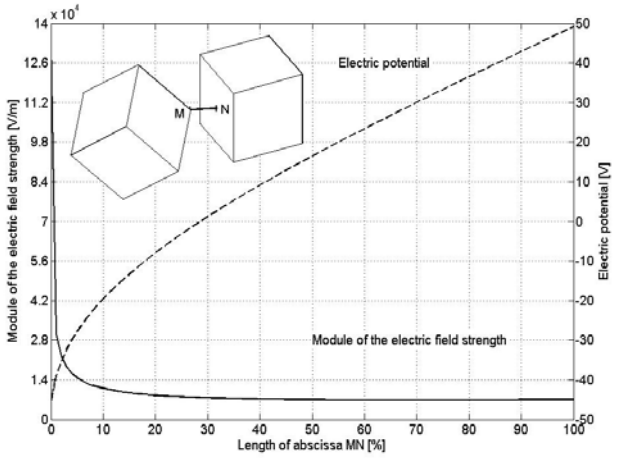

Fig. 8: Distribution of electric field quantities along the abscissa 5–6 (Fig. 5)

It can be seen that the module of the electric field strength at point 6 (left cube in Fig. 5) tends to infinity that is in full accordance with the physical reality.

Tab. 1 shows the change of several integral quantities with growing number of elements covering the face.

number of elements in the face	total charge Q_1 (pC)	total charge Q_2 (pC)	total capacitance C (pF)
36	-122.3	122.7	1.225
64	-122.6	123.0	1.228
100	-122.7	123.1	1.229
144	-122.8	123.2	1.230
196	-122.8	123.2	1.230
256	-122.9	123.2	1.231
324	-122.9	123.2	1.231
400	-122.9	123.3	1.231

Tab. 1: Convergence of the total charges on both cubes and the capacitance of the system

The total charges of both cubes Q_1 (left cube) and Q_2 (right cube) were calculated from (3) with the condition

that the total charge of the system equals zero. The capacitance C is then calculated as

$$C = \frac{\frac{1}{2}\left(|Q_1| + |Q_2|\right)}{\varphi_2 - \varphi_1} \tag{11}$$

The table shows that the convergence of the above integral methods is very fast. The total charges on both cubes converge to values $-1.23 \cdot 10^{-10}$ and $1.23 \cdot 10^{-10}$ C, respectively, the capacitance to $1.23 \cdot 10^{-12}$ F.

4 CONCLUSION

The paper (that represents natural continuation of [3]) brings more accurate results due to nonuniform discretization of the particular faces, better respecting real distribution of the surface electric charge that tends to infinity along all edges of both cubes. Next work in the field will be aimed at application of the Galerkin technique (substitution of the electric charge in particular cells by polynomials with suitably selected coefficients) that is assumed to bring still better results with the same (or even lower) number of the degrees of freedom.

5 ACKNOWLEDGMENT

Financial support of the Research Plan MSM 4977751310 and grant project GA ČR 102/05/0629 is gratefully acknowledged.

6 REFERENCES

[1] Harrington, R. F.: *Field Computations by Moment Methods*. IEEE Press, Piscataway, New Jersey, 1993.

[2] McWhirter, J. H., Duffin, R. J., Brehm, P. J.: *Computational Methods for Solving Static Field and Eddy Current Problems via Fredholm Integral Equations*. IEEE Trans. Mag., Vol. 15, 1979. pp. 1075–1084.

[3] Hamar, R., Doležel, I., Ulrych, B.: *Integral Solution of Electrostatic Fields in 3D Arrangements*. Proc. AMTEE'2003, Pilsen, 2003, CR, pp. A37–A42.

Ing. Roman Hamar, Ph.D.
University of West Bohemia
Faculty of Electrical Engineering
Univerzitní 26
306 14 Plzeň
E-mail: hamar@kte.zcu.cz

Prof. Ing. Ivo Doležel, CSc.
Czech Technical University
Faculty of Electrical Engineering
Technická 2
166 27 Praha 6
E-mail: dolezel@fel.cvut.cz